

## Electronic Supplementary Information

# Ultra-low loading Pt atomic cluster electrode with Pt-O bond as an active site with the high hydrogen evolution reaction performance

*Zhandong Ren,<sup>\*a</sup> Zhiqiang Xie,<sup>a</sup> Li Deng,<sup>a</sup> Chen Dong,<sup>a</sup> Guocan Song,<sup>a</sup> Xiaohui Liu<sup>a</sup>*

*Juanjuan Han,<sup>a</sup> Lin Zhuang,<sup>b</sup> Yi Liu<sup>c</sup> and Yuchan Zhu<sup>\*a</sup>*

a. School of Chemical and Environmental Engineering, Wuhan Polytechnic University, Wuhan, 430023, P. R. China.

b. College of Chemistry and Molecular Sciences, Hubei Key Lab of Electrochemical Power Sources, Wuhan University, Wuhan, 430072, PR China.

c. State Key Laboratory of Separation Membranes and Membrane Processes, School of Chemistry, Tiangong University, Tianjin 300387, P. R. China.

\* Corresponding author:

Zhandong Ren, Professor, School of Chemical and Environmental Engineering, Wuhan Polytechnic University, Wuhan, 430023, P. R. China. E-mail: [zhuyuchan@163.com](mailto:zhuyuchan@163.com). Tel.: 86-27-83943956.

Yuchan Zhu, Professor, School of Chemical and Environmental Engineering, Wuhan Polytechnic University, Wuhan, 430023, P. R. China. E-mail: [zhuyuchan@163.com](mailto:zhuyuchan@163.com). Tel.: 86-27-83943956.

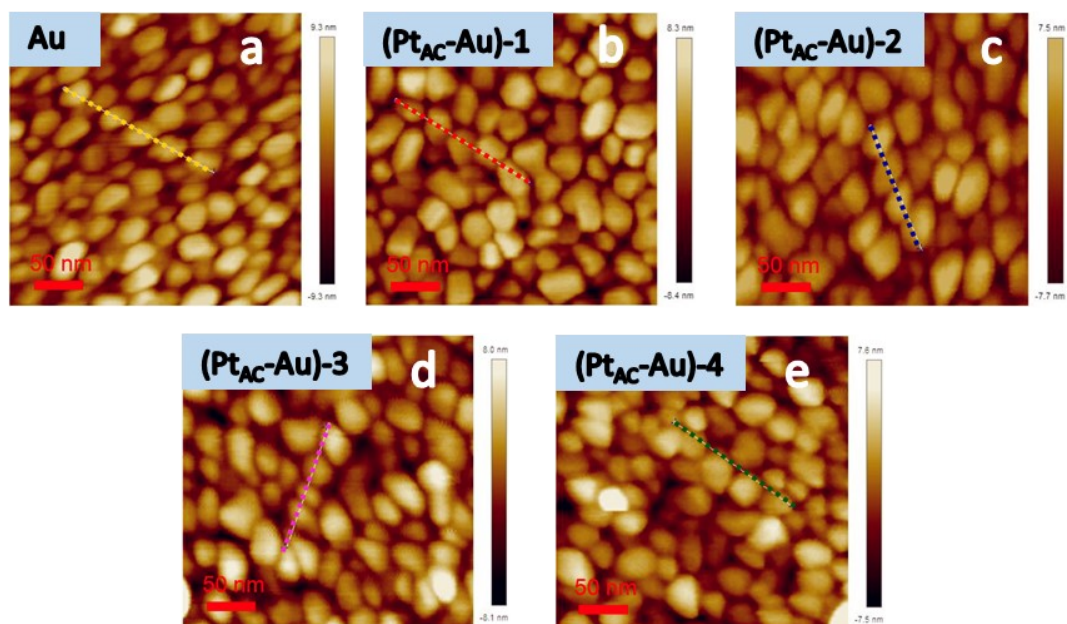


**Figure S1** AFM images of Au and (Pt<sub>AC</sub>-Au)-x (x=1, 2, 3, 4) with different Pt loading (Au (a), (Pt<sub>AC</sub>-Au)-1 (b), (Pt<sub>AC</sub>-Au)-2 (c), (Pt<sub>AC</sub>-Au)-3 (d) and (Pt<sub>AC</sub>-Au)-4 (e)).

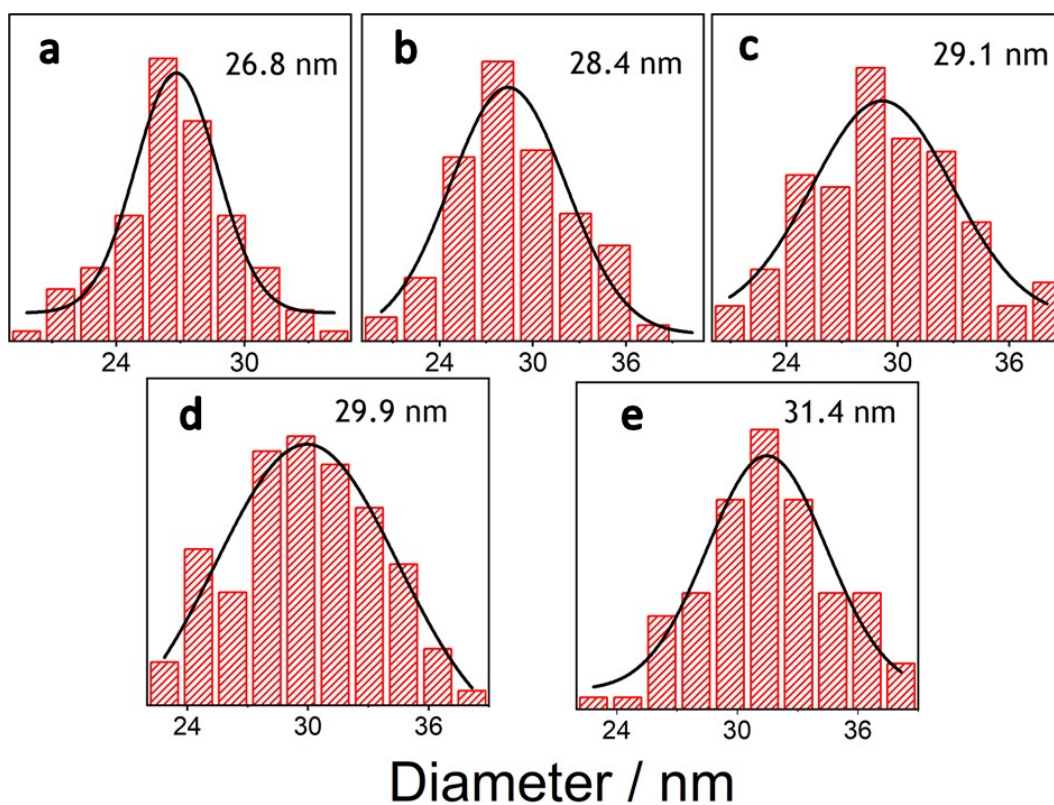


**Figure S2** The particle sizes of Au and (Pt<sub>AC</sub>-Au)-x (x=1, 2, 3, 4) with different Pt loading according to AFM image (Au (a), (Pt<sub>AC</sub>-Au)-1 (b), (Pt<sub>AC</sub>-Au)-2 (c), (Pt<sub>AC</sub>-Au)-3 (d) and (Pt<sub>AC</sub>-Au)-4 (e)).

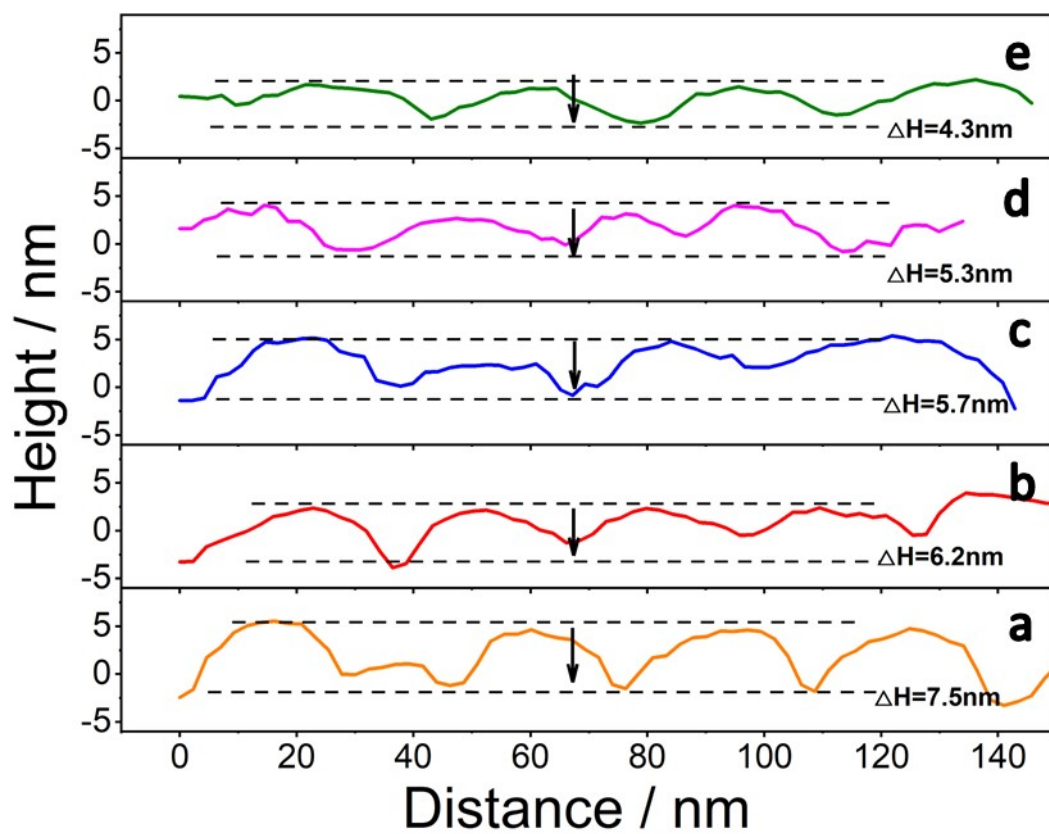


**Figure S3** The height differences of Au and  $(\text{Pt}_{\text{AC}}\text{-Au})\text{-}x$  ( $x=1, 2, 3, 4$ ) with different Pt loading according to AFM image (Au (a),  $(\text{Pt}_{\text{AC}}\text{-Au})\text{-}1$  (b),  $(\text{Pt}_{\text{AC}}\text{-Au})\text{-}2$  (c),  $(\text{Pt}_{\text{AC}}\text{-Au})\text{-}3$  (d) and  $(\text{Pt}_{\text{AC}}\text{-Au})\text{-}4$  (e)).

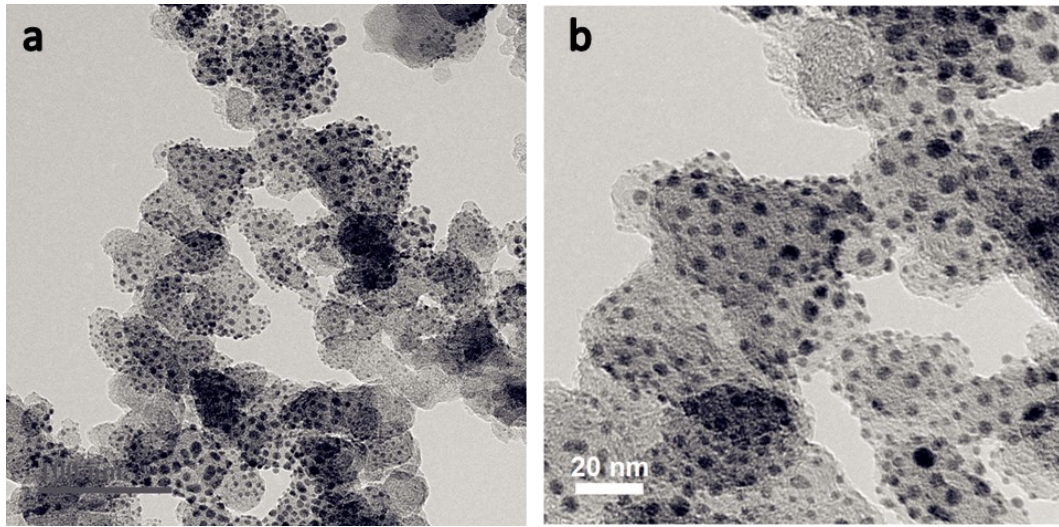


**Figure S4** The TEM images of the (Pt<sub>AC</sub>-Au)-1 electrode.

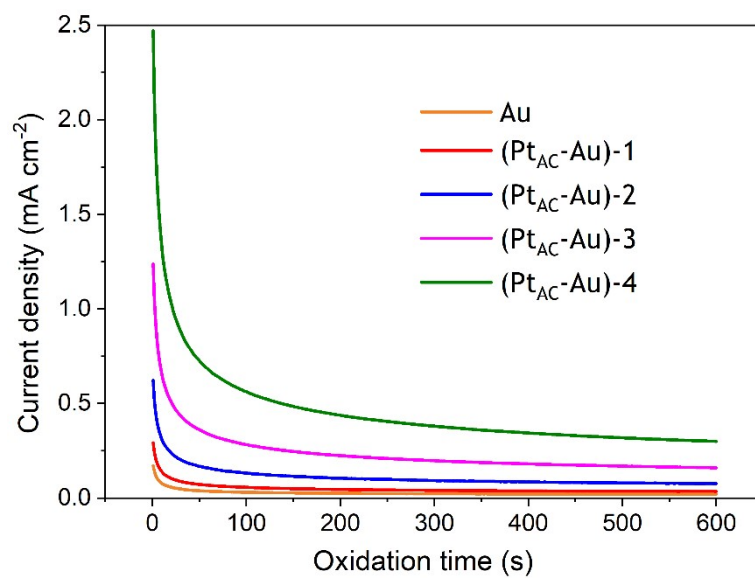


**Figure S5** The anode oxidation curves of Au and (Pt<sub>AC</sub>-Au)-x (x=1, 2, 3, 4) electrodes with different Pt loading at 1.7 V.



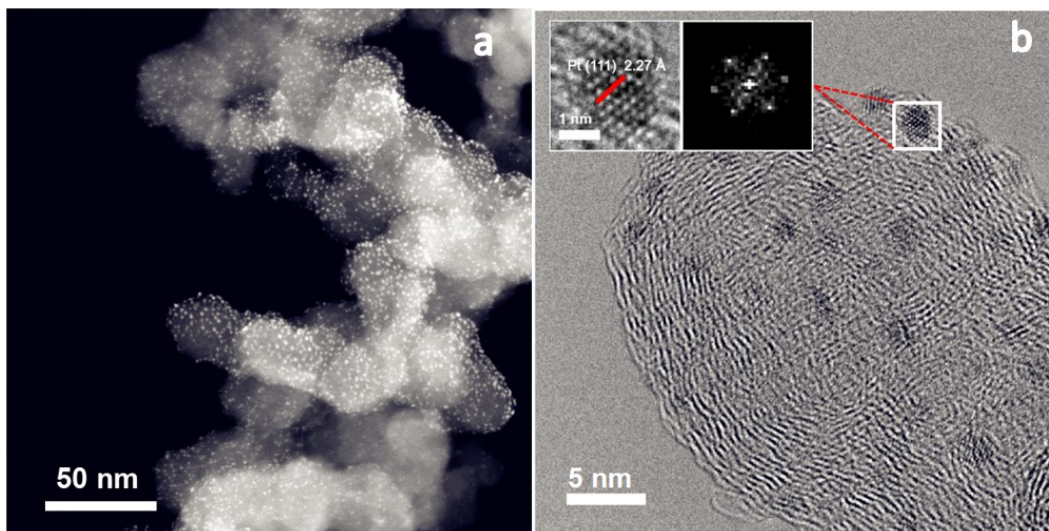


**Figure S6** The HAADF-STEM (a) and HRTEM (b) of the Pt-1 electrode.

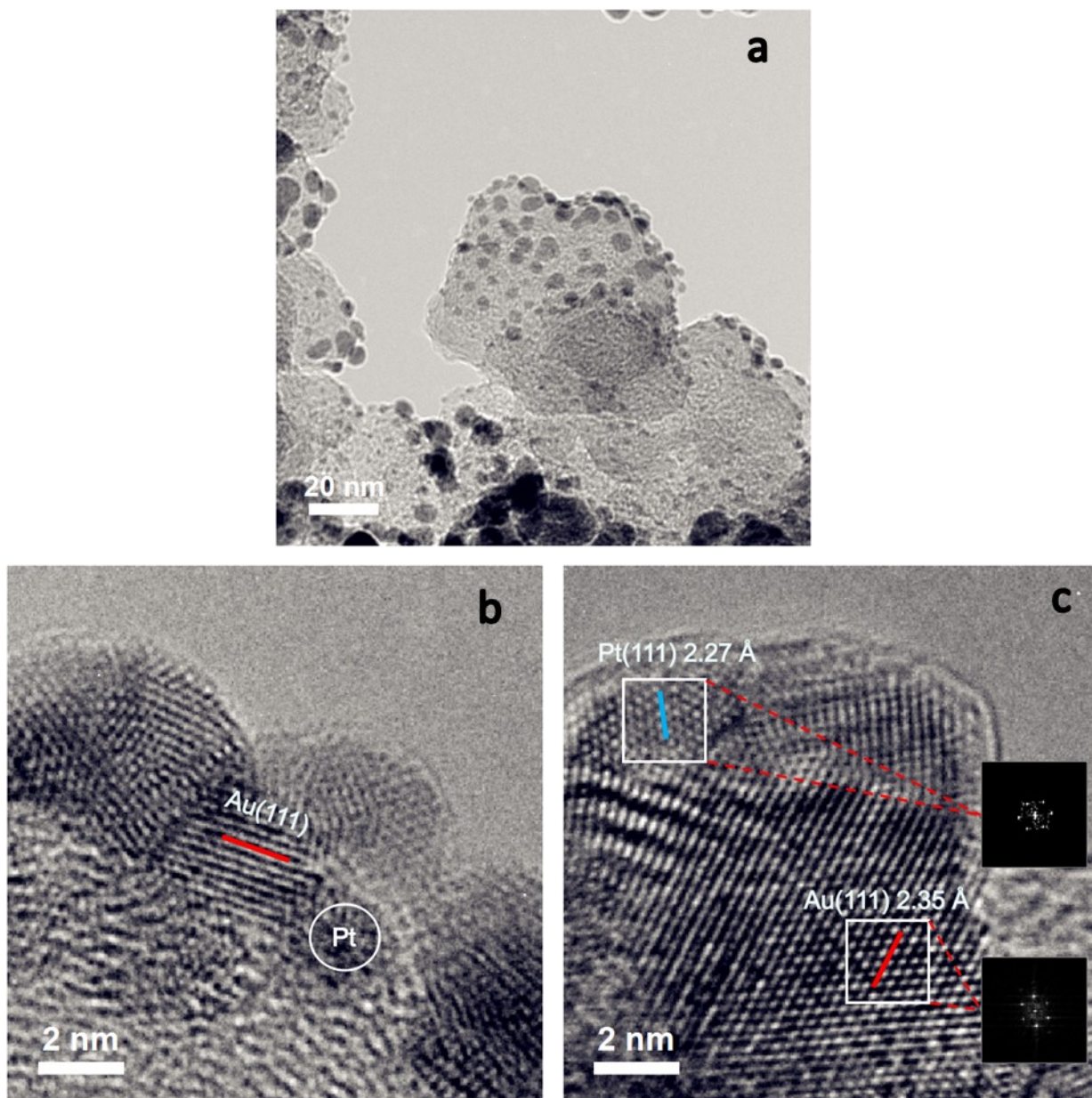


**Figure S7** The TEM (a) and HRTEM (b, c) images of the (Pt<sub>AC</sub>-Au)-4 electrode.



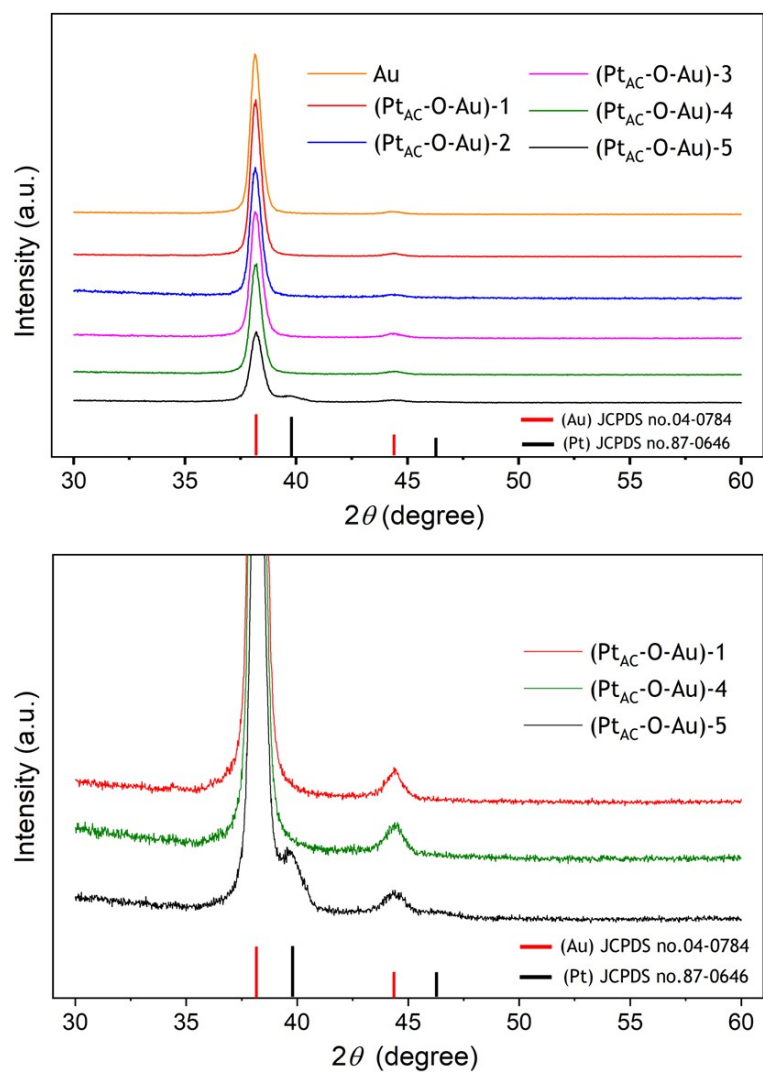


**Figure S8** XRD diagrams of Au and (Pt<sub>AC</sub>-O-Au)-x (x=1, 2, 3, 4, 5) with different Pt loading.

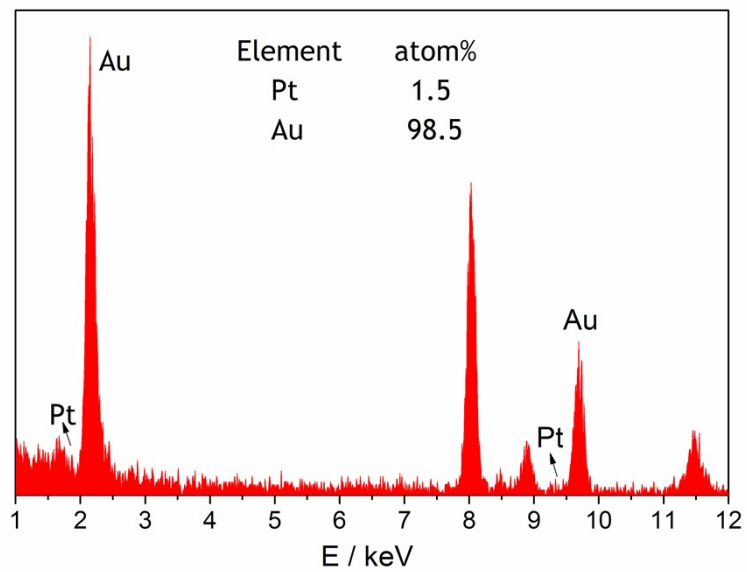


**Figure S9** The EDS element analysis of (Pt<sub>AC</sub>-Au)-1 electrode.

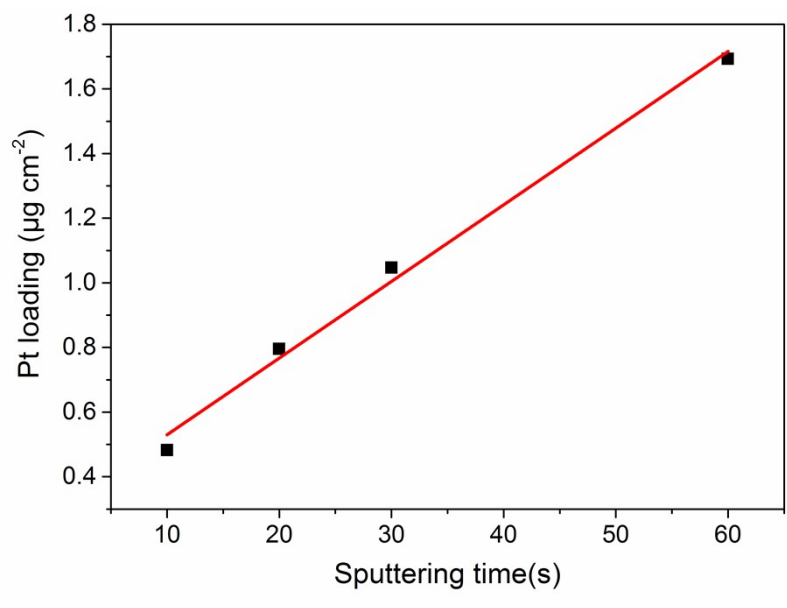


**Figure S10** Relationship between the sputtering time and Pt loading

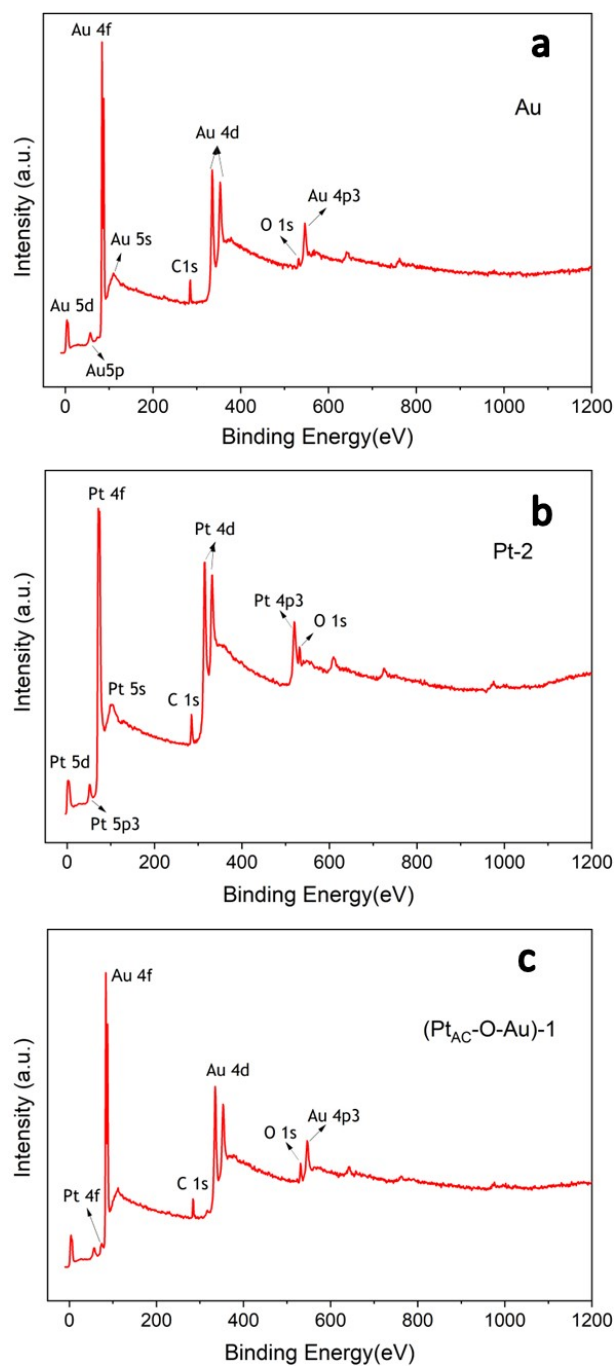


**Figure S11** The survey XPS analysis of the Au (a), Pt-2 (b) and (Pt<sub>AC</sub>-O-Au)-1 (c) electrodes.

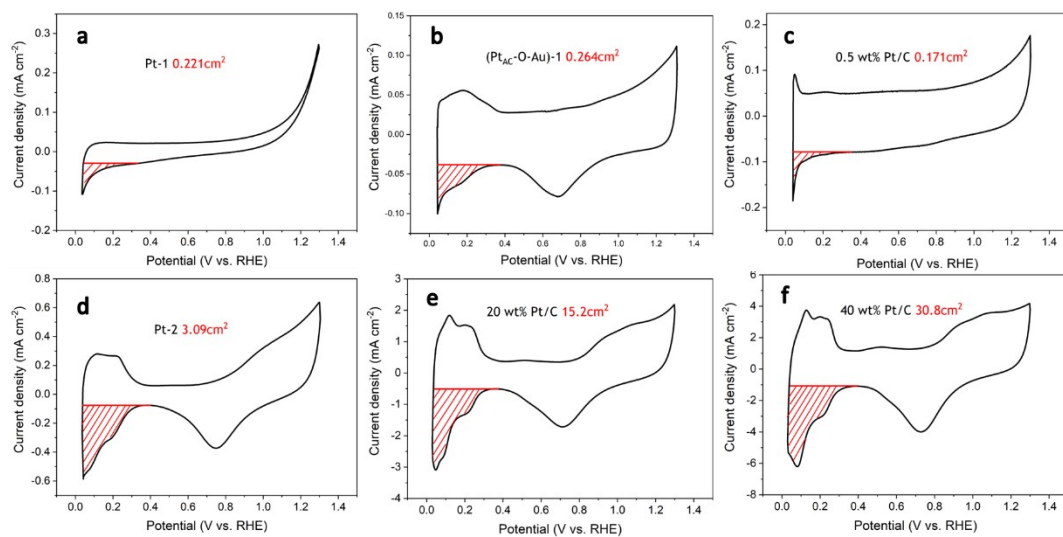


**Figure S12** Cyclic voltammograms of Pt-1 (a), (Pt<sub>AC</sub>-O-Au)-1 (b), 0.5 wt% Pt/C (c), Pt-2 (d), 40 wt% Pt/C (e) and 20 wt% Pt/C (f).



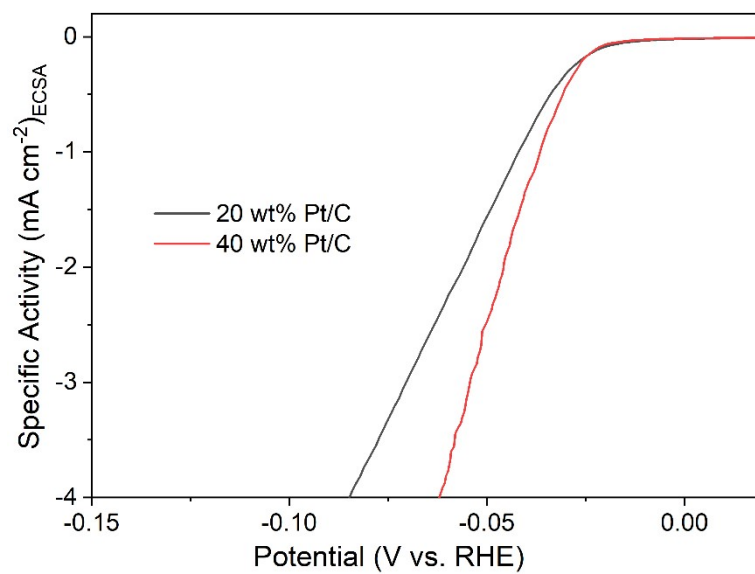


**Figure S13** The specific activities (SAs) of 20 wt% Pt/C and 40 wt% Pt/C.

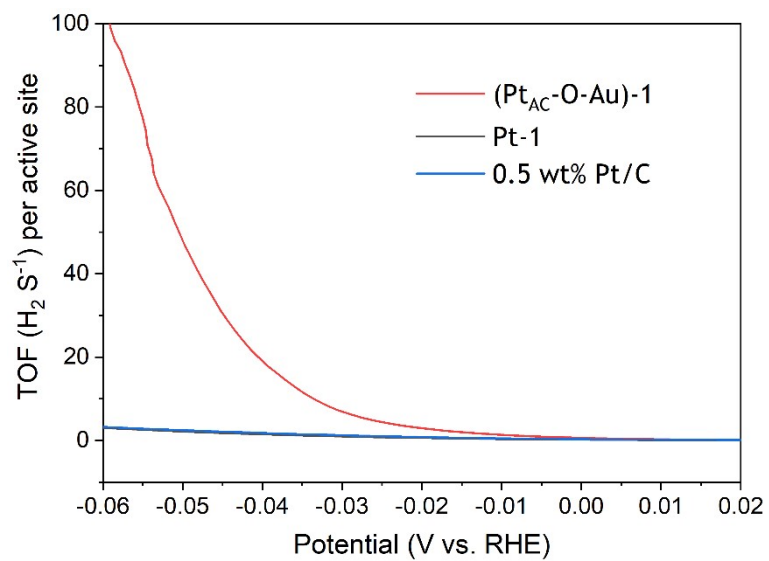


**Figure S14** The turnover frequency (TOF) of  $(\text{Pt}_{\text{AC}}\text{-O-Au})\text{-1}$ , Pt-1 and 0.5 wt% Pt/C.

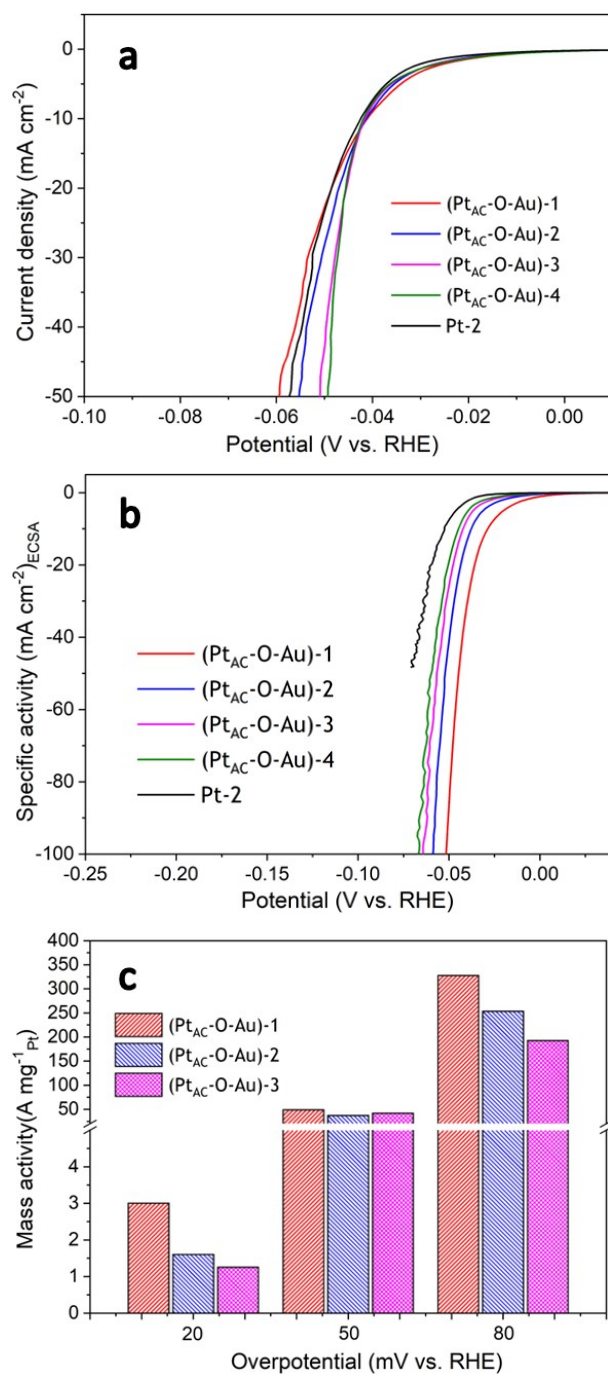


**Figure S15** HER apparent activity (a), specific activity (b) and mass specific activity (c) of (Pt<sub>AC</sub>-O-Au)-x (x=1, 2, 3, 4) with different Pt loading.

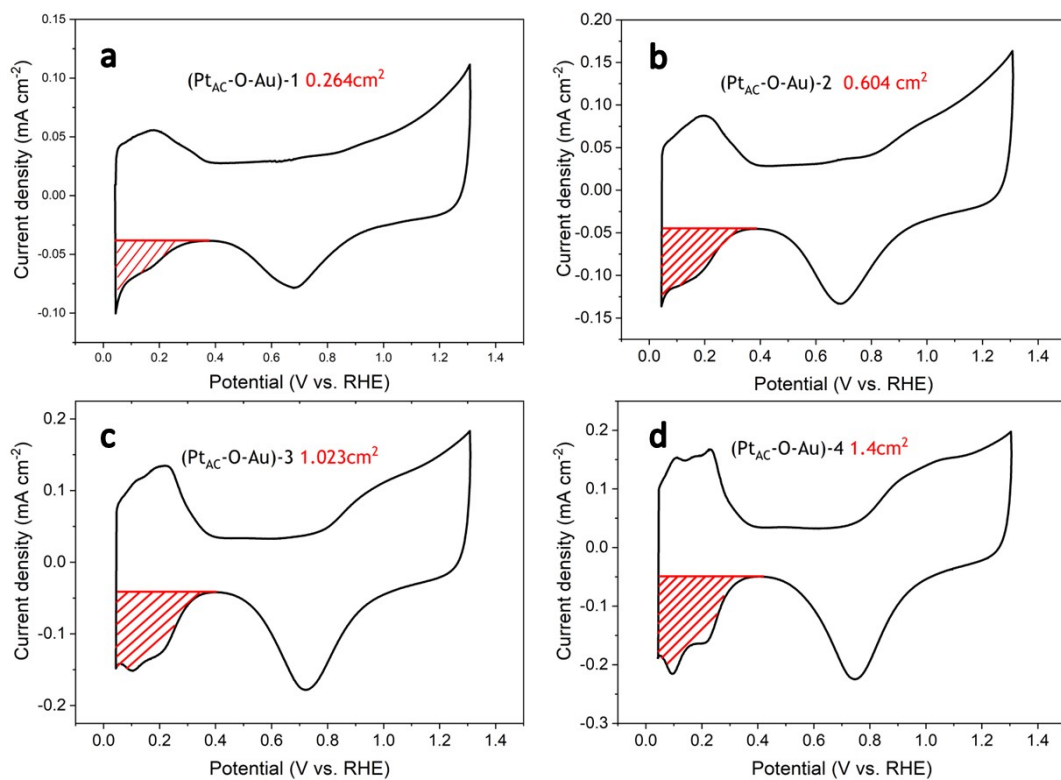


**Figure S16** Cyclic voltammograms of (Pt<sub>AC</sub>-O-Au)-1 (a), (Pt<sub>AC</sub>-O-Au)-2 (b), (Pt<sub>AC</sub>-O-Au)-3 (c) and (Pt<sub>AC</sub>-O-Au)-4 (d).

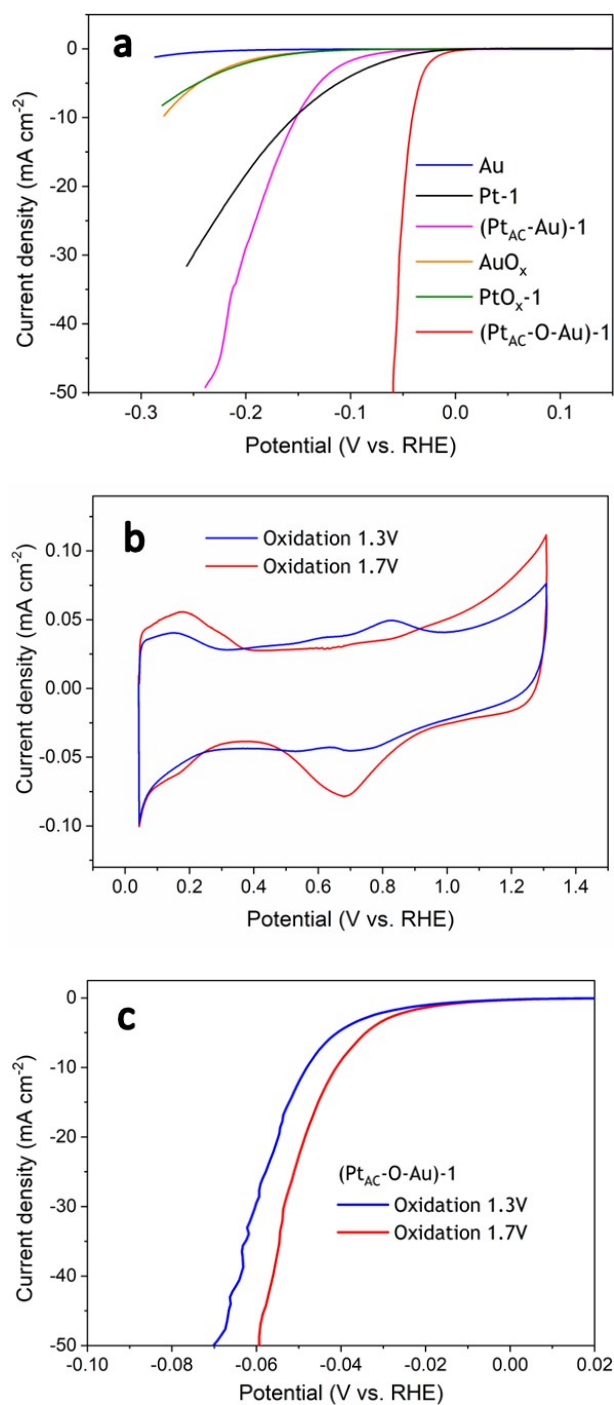


**Figure S17** The apparent activity of (Pt<sub>AC</sub>-O-Au)-1, (Pt<sub>AC</sub>-Au)-1, PtO<sub>x</sub>-1, Pt-1, AuO<sub>x</sub> and Au (a). Cyclic voltammograms (b) and linear sweep voltammetry curves (c) of (Pt<sub>AC</sub>-O-Au)-1 at anodic oxidation potentials of 1.3 and 1.7 V.



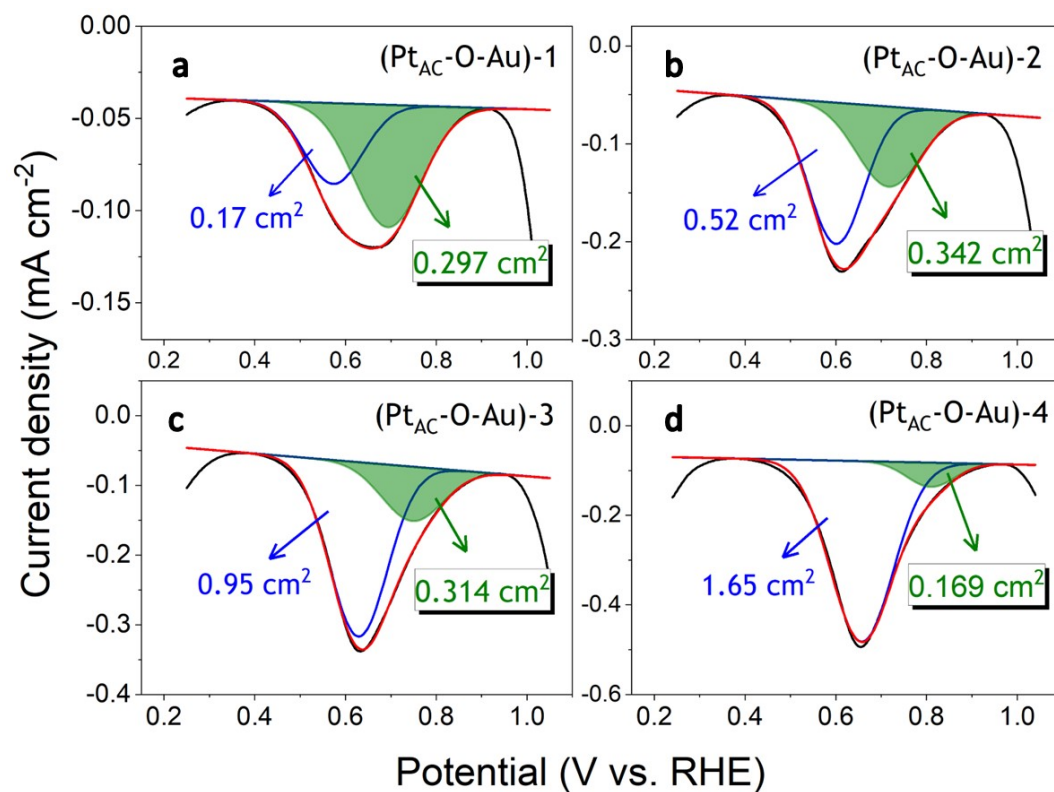


**Figure S18** Peak fitting of Au-O-Pt and PtO<sub>x</sub> reduction peaks of (Pt<sub>AC</sub>-O-Au)-1 (a), (Pt<sub>AC</sub>-O-Au)-2 (b), (Pt<sub>AC</sub>-O-Au)-3 (c) and (Pt<sub>AC</sub>-O-Au)-4 (d).

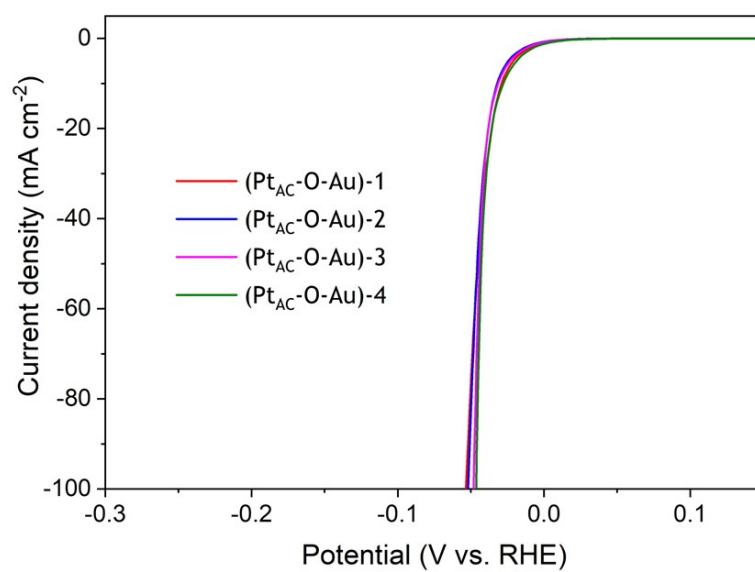


**Figure S19** The specific activity of (Pt<sub>AC</sub>-O-Au)-x (x=1, 2, 3, 4) with different Pt loading (The calculation of ECSA is based on the reduction peak area of Au-O-Pt at 0.72V).

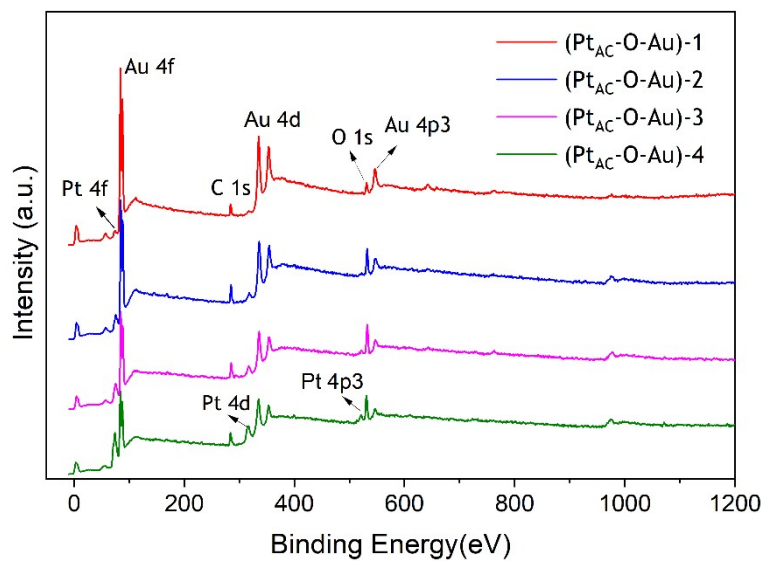


**Figure S20** The survey XPS analysis of the (Pt<sub>AC</sub>-Au)-x (x=1, 2, 3, 4) electrodes with different Pt loading.

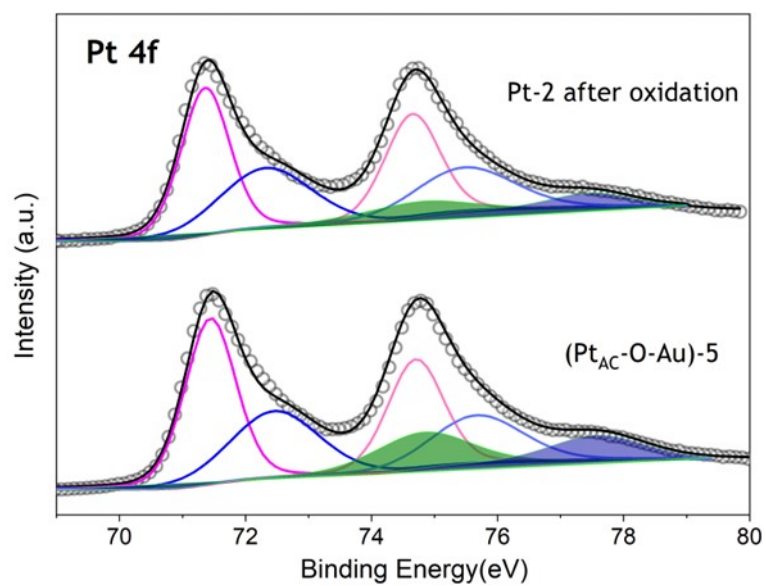


**Figure S21** The XPS core-level spectra of Pt 4f obtained from the (Pt<sub>AC</sub>-O-Au)-5 and Pt-2 (after oxidation) electrodes.

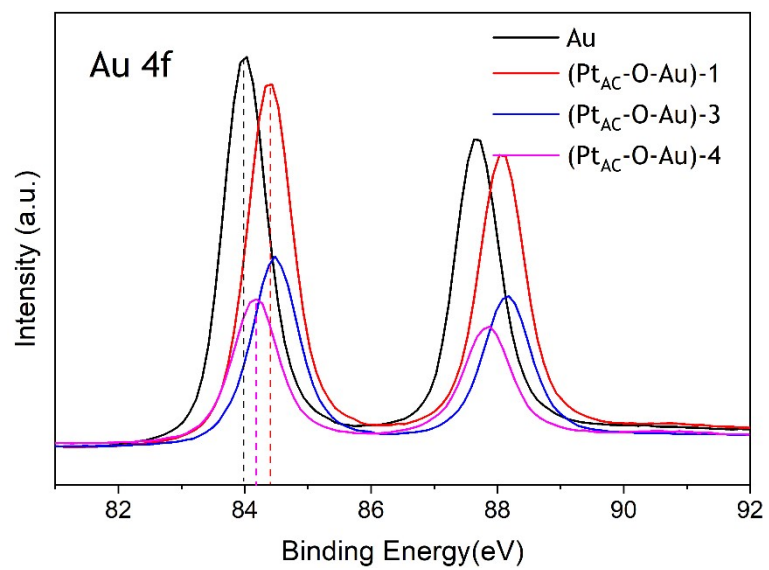


**Figure S22** The XPS core-level spectra of Au 4f obtained from Au and (Pt<sub>AC</sub>-Au)-x (x=1, 3, 4) electrodes with different Pt loading.



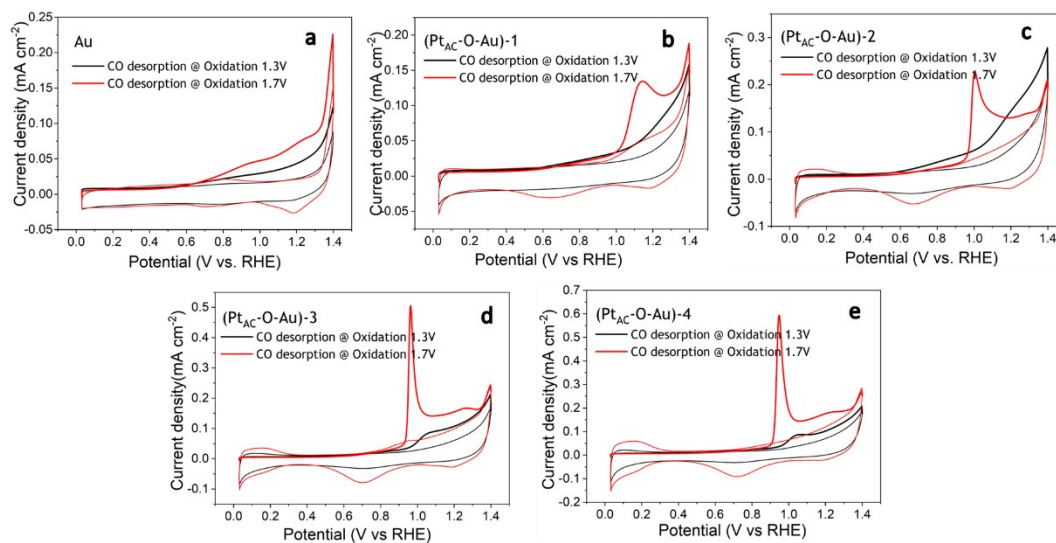


**Figure S23** The CO adsorption-stripping curves of (Pt<sub>AC</sub>-Au)-x (x=1, 2, 3, 4) electrodes with anodic oxidation potential at 1.3 V and 1.7 V (Au (a), (Pt<sub>AC</sub>-Au)-1 (b), (Pt<sub>AC</sub>-Au)-2 (c), (Pt<sub>AC</sub>-Au)-3 (d) and (Pt<sub>AC</sub>-Au)-4 (e)).

## Supplementary Tables

**Table S1** Pt loading with different sputtering times using ICP-OES

Sputteri ng time(s)	Electrode	Pt( $\mu\text{g cm}^{-2}$ )	Au( $\mu\text{g cm}^{-2}$ )	Pt(atom%)
10	(Pt <sub>AC</sub> -O-Au)-1	0.482	100	0.484
20	(Pt <sub>AC</sub> -O-Au)-2	0.795	104	0.766
30	(Pt <sub>AC</sub> -O-Au)-3	1.047	109	0.961
60	(Pt <sub>AC</sub> -O-Au)-4	1.693	101	1.664
600	(Pt <sub>AC</sub> -O-Au)-5	17.58	105	14.44

**Table S2** Pt loading with different sputtering times using XPS

Sputtering time(s)	Electrode	Pt(atom%)	Au(atom%)
	Au		100
10	(Pt <sub>AC</sub> -O-Au)-1	4.79	95.21
20	(Pt <sub>AC</sub> -O-Au)-2	15.3	84.7
30	(Pt <sub>AC</sub> -O-Au)-3	23.9	76.1
60	(Pt <sub>AC</sub> -O-Au)-4	42.4	57.6
600	(Pt <sub>AC</sub> -O-Au)-5	99	1

**Table S3** The Pt loading capacity, apparent activity and mass specific activity of different low Pt loading electrocatalysts in the references and this work.

Electrodes	Loading ( $\mu\text{g}_{\text{Pt}} \text{cm}^{-2}$ )	$\eta$ at 10 mA $\text{cm}^{-2}$ (mV)	Mass activity ( $\text{A mg}^{-1}$ )	Tafel slope ( $\text{mv dec}^{-1}$ )	Ref
Pt/VS <sub>2</sub> /CP	379.2	77	22.88 @ 200mV	39.46	1
Pt/Ni-Mo-N-O	243.75	89.5@100	10.05 @ 134mV	31.5	2
Pt-a-MoS <sub>3</sub> NDs	84.99	11.5	3.23 @ 20mV	25.4	3
Pt SASs/AG	31.1	12	22.4 @ 50mV	29.33	4
Pt/WO <sub>3</sub> -600	29.94	8	7.015 @ 50mV	35	5
Pt <sub>doped</sub> @WC <sub>x</sub>	22.9	2.4	14.28 @ 100mV	20	6
PtW NP s/C <sup>a</sup>	20.4	19.4	0.566 @ 20mV	27.8	7
Pt <sub>0.04</sub> /Ni-DA	17.72	19	2.13 @ 50mV	34	8
Pt/def-WO <sub>3</sub> @CFC	15.9	42	0.764 @ 50mV	61	9
Pt <sub>3</sub> Ni <sub>2</sub> NWs-S/C	15.0	~23	-----	-----	10
Pt@MoS <sub>2</sub> /NiS <sub>2</sub>	~13.68	34	-----	40	11
MXene/B-Pt	13.4	14	-----	78.6	12
Mo <sub>2</sub> TiC <sub>2</sub> T <sub>x</sub> -Pt <sub>SA</sub>	~12	30	8.3 @ 77mV	30	13
Pt-MoO <sub>2</sub> @PC	11.6	20	11.34 @ 50mV	22	14
Pt/TiO <sub>2</sub> -O <sub>V</sub>	10.45	18	14.82 @ 50mV	12	15
Pt/MOF-C	10.191	28	0.97 @ 50mV	24.4	16
Pt@VNC	9.802	5	-----	21	17
Pt <sub>1</sub> Ru <sub>1</sub> /NMHCS-A	9.58	22	3.49 @ 50mV	38	18
CDs/Pt-PANI	8.1	30	1.22 @ 30mV	41.7	19
Pt <sub>5</sub> /HMCS <sup>a</sup>	7.6	20.7	12.8 @ 30 mV	28.3	20
Pt <sub>1</sub> /N-C	6.25	19	-----	14.2	21
Pt <sub>at</sub> -CoP MNSs/CFC	5.89	13	-----	30.28	22
Pt@mh-3D MXene <sup>a</sup>	4.8	12	19.45 @ 100mV	24.2	23
Pt-GDY-2	4.65	~66	23.64 @ 100mV	46.6	24
Pt-HNCNT	~3.8	15	20.4 @ 50mV	29.1	25
0.66% Pt-WC/CNT	3.4	42	8.9 @ 50mV	-----	26
PtNC/S-C	2.55	11	26.1 @ 20mV	24	27
Ti <sub>3</sub> C <sub>2</sub> T <sub>x</sub> -Pt <sub>SA</sub>	2.38	38	23.21 @ 50mV	45	28

Pt Cs/MoO <sub>2</sub> NSs-L	1.79	47	7.43 @ 50mV	32.6	29
AL-Pt/Pd <sub>3</sub> Pb <sup>a</sup>	~1.6	13.8	7.834 @ 50mV	18	30
CNT/Pt@CdSe-OCPs	~1.58	-----	166.2 @ 150mV	61.3	31
Pt <sub>C</sub> (250)	1.41	37.4	107.7 @ 50mV	30	32
Pt-GT-1	1.4	15	-----	24	33
Pt-Ru dimer	1.38	50	23.1 @ 50mV	28.9	34
F-SnO <sub>2</sub> @Pt	1.2	42	≈10 @ 50mV	34	35
CoPt-Pt <sub>SA</sub> /NDPCF	1.18	31	74.31 @ 50mV	43.65	36
Pt-Ti <sub>x</sub> C	1	24.9	49.69 @ 50mV	22.3	37
Pt/MPNC	0.9	18.6±1.6	56±3 @ 50mV	-----	38
Pt SA/m-WO <sub>3-x</sub>	0.86	47	12.8 @ 50mV	45	39
Pt-SAs/CoNC	0.45	57	18.8 @ 50mV	64.5	40
Pt-SAs/WS <sub>2</sub>	0.415	32	54 @ 100 mV	28	41
PtO <sub>x</sub> /TiO <sub>2</sub>	~0.21	~110	8.68 @ 50mV	40	42
Pt/TiB <sub>x</sub> O <sub>y</sub>	0.191	-----	37.8 @ 50mV	32	43
(Pt <sub>AC</sub> -O-Au)-1	0.48	41	3.02 @ 20mV 49.2 @ 50mV 329 @ 80mV	28.6	This work

## References

- (1) J. Zhu, L. Cai, X. Yin, Z. Wang, L. Zhang, H. Ma, Y. Ke, Y. Du, S. Xi, A. Wee, Y. Chai, W. Zhang, Enhanced Electrocatalytic Hydrogen Evolution Activity in Single-Atom Pt-Decorated VS<sub>2</sub> Nanosheets, *ACS Nano*, 2020, 14, 5600–5608.
- (2) W. Yu, Z. Chen, Y. Fu, W. Xiao, B. Dong, Y. Chai, Z. Wu, L. Wang, Superb All-pH Hydrogen Evolution Performances Powered by Ultralow Pt-Decorated Hierarchical Ni-Mo Porous Microcolumns, *Adv. Funct. Mater.*, 2023, 33, 2210855.
- (3) K. Guo, J. Zheng, J. Bao, Y. Li, D. Xu, Combining Highly Dispersed Amorphous MoS<sub>3</sub> with Pt Nanodendrites as Robust Electrocatalysts for Hydrogen Evolution Reaction, *Small*, 2023, 19, 2208077.
- (4) S. Ye, F. Luo, Q. Zhang, P. Zhang, T. Xu, Q. Wang, D. He, L. Guo, Y. Zhang, C. He, X. Ouyang, M. Gu, J. Liu, X. Sun, Highly stable single Pt atomic sites anchored on aniline-stacked graphene for hydrogen evolution reaction, *Energy Environ. Sci.* **2019**, 12, 1000-1007.
- (5) X. Fan, C. Liu, B. Gao, H. Li, Y. Zhang, H. Zhang, Q. Gao, X. Cao, Y. Tang, Electronic Structure Engineering of Pt Species over Pt/WO<sub>3</sub> toward Highly Efficient Electrocatalytic Hydrogen Evolution, *Small*, 2023, 2301178. <https://doi.org/10.1002/smll.202301178>
- (6) T. Ma, H. Cao, S. Li, S. Cao, Z. Zhao, Z. Wu, R. Yan, C. Yang, Y. Wang, P. A. Aken, L. Qiu, Y.-G. Wang, C. Cheng, Crystalline Lattice-Confined Atomic Pt in Metal Carbides to Match Electronic Structures and Hydrogen Evolution Behaviors of Platinum, *Adv. Mater.*, 2022, 34, 2206368



- (7) D. Kobayashi, H. Kobayashi, D. Wu, S. Okazoe, K. Kusada, T. Yamamoto, T. Toriyama, S. Matsumura, S. Kawaguchi, Y. Kubota, S. M. Aspera, H. Nakanishi, S. Arai, H. Kitagawa, Significant Enhancement of Hydrogen Evolution Reaction Activity by Negatively Charged Pt through Light Doping of W, *J. Am. Chem. Soc.* **2020**, *142*, 17250–17254.
- (8) Y. Peng, K. Ma, T. Xie, J. Du, L. Zheng, F. Zhang, X. Fan, W. Peng, J. Ji, Yang Li, Tunable Pt–Ni Interaction Induced Construction of Disparate Atomically Dispersed Pt Sites for Acidic Hydrogen Evolution, *ACS Appl. Mater. Interfaces*, **2023**, *15*, 27089–27098.
- (9) H. Tian, X. Cui, L. Zeng, L. Su, Y. Song, J. Shi, Oxygen vacancy-assisted hydrogen evolution reaction of the Pt/WO<sub>3</sub> electrocatalyst, *J. Mater. Chem. A*, **2019**, *7*, 6285–6293.
- (10) P. Wang, X. Zhang, J. Zhang, S. Wan, S. Guo, G. Lu, J. Yao, X. Huang, Precise Tuning in Platinum–Nickel/Nickel Sulfide Interface Nanowires for Synergistic Hydrogen Evolution Catalysis, *Nat. Commun.* **2017**, *8*, 14580.
- (11) Y. Guan, Y. Feng, J. Wan, X. Yang, L. Fang, X. Gu, R. Liu, Z. Huang, J. Li, J. Luo, C. Li, Y. Wang, Ganoderma-Like MoS<sub>2</sub>/NiS<sub>2</sub> with Single Platinum Atoms Doping as an Efficient and Stable Hydrogen Evolution Reaction Catalyst, *Small*, **2018**, *14*, 1800697.
- (12) X. Zhao, M. Chen, Y. Zhou, H. Zhang, G. Hu, Fluorinated Mxenes accelerate the hydrogen evolution activity of in situ induced snowflake-like nano-Pt, *J. Mater. Chem. A*, **2023**, *11*, 5830–5840.
- (13) J. Zhang, Y. Zhao, X. Guo, C. Chen, C.-L. Dong, R.-S. Liu, C.-P. Han, Y. Li, Y. Gogotsi, G. Wang, Single platinum atoms immobilized on an MXene as an efficient catalyst for the hydrogen evolution reaction, *Nat. Catal.*, **2018**, *1*, 985–992.
- (14) Y. Jiang, M. Yang, M. Qu, Y. Wang, Z. Yang, Q. Feng, X. Deng, W. Shen, M. Li, R. He, *In situ* confinement of Pt within three-dimensional MoO<sub>2</sub>@porous carbon for efficient hydrogen evolution, *J. Mater. Chem. A*, **2020**, *8*, 10409–10418.
- (15) Z. Wu, P. Yang, Q. Li, W. Xiao, Z. Li, G. Xu, F. Liu, B. Jia, T. Ma, S. Feng, L. Wang, Microwave Synthesis of Pt Clusters on Black TiO<sub>2</sub> with Abundant Oxygen Vacancies for Efficient Acidic Electrocatalytic Hydrogen Evolution, *Angew. Chem. Int. Ed.*, **2023**, *62*, e202300406.
- (16) M. Wang, Y. Xu, C.-K. Peng, S.-Y. Chen, Y.-G. Lin, Z. Hu, L. Sun, S. Ding, C.-W. Pao, Q. Shao, X. Huang, Site-Specified Two-Dimensional Heterojunction of Pt Nanoparticles/Metal–Organic Frameworks for Enhanced Hydrogen Evolution, *J. Am. Chem. Soc.*, **2021**, *143*, 16512–16518.
- (17) H. Jin, M. Ha, M. G. Kim, J. H. Lee, K. S. Kim, Engineering Pt Coordination Environment with Atomically Dispersed Transition Metal Sites Toward Superior Hydrogen Evolution, *Adv. Energy Mater.*, **2023**, *13*, 2204213.
- (18) W. Zhao, C. Luo, Y. Lin, G.-B. Wang, H. M. Chen, P. Kuang, J. Yu, Pt–Ru Dimer Electrocatalyst with Electron Redistribution for Hydrogen Evolution Reaction, *ACS Catal.*, **2022**, *12*, 5540–5548.
- (19) Q. Dang, Y. Y. Sun, X. Wang, W. X. Zhu, Y. Chen, F. Liao, H. Huang, M. W. Shao, Carbon dots–Pt modified polyaniline nanosheet grown on carbon cloth as stable and high-efficient electrocatalyst for hydrogen evolution in pH-universal electrolyte, *Appl. Catal. B-Environ.*, **2019**, *257*, 117905.
- (20) X.-K. Wan, H. B. Wu, B. Y. Guan, D. Luan, X. W. (David) Lou, Confining Sub-Nanometer Pt Clusters in Hollow Mesoporous Carbon Spheres for Boosting Hydrogen Evolution Activity, *Adv. Mater.*, **2020**, *32*, 1901349.
- (21) S. Fang, X. Zhu, X. Liu, J. Gu, W. Liu, D. Wang, W. Zhang, Y. Lin, J. Lu, S. Wei, Y. Li, T. Yao, Uncovering near-free platinum single-atom dynamics during electrochemical hydrogen evolution reaction, *Nat. Commun.*, **2020**, *11*, 1029.
- (22) S. Ye, W. Xiong, P. Liao, L. Zheng, X. Ren, C. He, Q. Zhang, J. Liu, Removing the barrier to water dissociation on single-atom Pt sites decorated with a CoP mesoporous nanosheet array to achieve improved hydrogen evolution, *J. Mater. Chem. A*, **2020**, *8*, 11246–11254.

- (23) L. Xiu, W. Pei, S. Zhou, Z. Wang, P. Yang, J. Zhao, J. Qiu, Multilevel Hollow MXene Tailored Low-Pt Catalyst for Efficient Hydrogen Evolution in Full-pH Range and Seawater, *Adv. Funct. Mater.*, **2020**, *30*, 1910028.
- (24) X.-P. Yin, H.-J. Wang, S.-F. Tang, X.-L. Lu, M. Shu, R. Si, T.-B. Lu, Engineering the Coordination Environment of Single-Atom Platinum Anchored on Graphdiyne for Optimizing Electrocatalytic Hydrogen Evolution, *Angew. Chem. Int. Ed.*, **2018**, *57*, 9382-9386.
- (25) L. Zhang, Q. Wang, R. Si, Z. Song, X. Lin, M. N. Banis, K. Adair, J. Li, K. Doyle-Davis, R. Li, L.-M. Liu, M. Gu, X. Sun, New Insight of Pyrrole-Like Nitrogen for Boosting Hydrogen Evolution Activity and Stability of Pt Single Atoms, *Small*, **2021**, *17*, 2004453.
- (26) Y. Chu, R. Peng, Z. Chen, L. Li, F. Zhao, Y. Zhu, S. Tong, H. Zheng, Modulating Dominant Facets of Pt through Multistep Selective Anchored on WC for Enhanced Hydrogen Evolution Catalysis, *ACS Appl. Mater. Interfaces*, **2023**, *15*, 9263–9272.
- (27) Q.-Q. Yan, D.-X. Wu, S.-Q. Chu, Z.-Q. Chen, Y. Lin, M.-X. Chen, J. Zhang, X.-J. Wu, H.-W. Liang, Reversing the charge transfer between platinum and sulfur-doped carbon support for electrocatalytic hydrogen evolution. *Nat. Commun.*, **2019**, *10*, 4977.
- (28) J. Zhang, E. Wang, S. Cui, S. Yang, X. Zou, Y. Gong, Single-Atom Pt Anchored on Oxygen Vacancy of Monolayer Ti<sub>3</sub>C<sub>2</sub>T<sub>x</sub> for Superior Hydrogen Evolution, *Nano Lett.*, **2022**, *22*, 1398–1405.
- (29) X. Li, J. Y. Yu, J. Jia, A. Z. Zhao, L. L. Zhao, T. L. Xiong, H. Liu and W. J. Zhou, Confined distribution of platinum clusters on MoO<sub>2</sub> hexagonal nanosheets with oxygen vacancies as a high-efficiency electrocatalyst for hydrogen evolution reaction, *Nano Energy*, **2019**, *62*, 127-135.
- (30) Y. Yao, X.-K. Gu, D. He, Z. Li, W. Liu, Q. Xu, T. Yao, Y. Lin, H.-J. Wang, C. Zhao, X. Wang, P. Yin, H. Li, X. Hong, S. Wei, W.-X. Li, Y. Li, Y. Wu, Engineering the Electronic Structure of Submonolayer Pt on Intermetallic Pd<sub>3</sub>Pb via Charge Transfer Boosts the Hydrogen Evolution Reaction, *J. Am. Chem. Soc.*, **2019**, *141*, 19964–19968.
- (31) L. Najafi, S. Bellani, A. Castelli, M. P. Arciniegas, R. Brescia, R. Oropesa-Nuñez, B. Martín-García, M. Serri, F. Drago, L. Manna, F. Bonaccorso, Octapod-Shaped CdSe Nanocrystals Hosting Pt with High Mass Activity for the Hydrogen Evolution Reaction, *Chem. Mater.*, **2020**, *32*, 2420–2429.
- (32) J.-F. Huang, R.-H. Zeng, J.-L. Chen, Thermostable carbon-supported subnanometer-sized (<1 nm) Pt clusters for the hydrogen evolution reaction, *J. Mater. Chem. A*, **2021**, *9*, 21972-21980.
- (33) J. N. Tiwari, S. Sultan, C. W. Myung, T. Yoon, N. Li, M. Ha, A. M. Harzandi, H. J. Park, D. Y. Kim, S. S. Chandrasekaran, W. G. Lee, V. Vij, H. Kang, T. J. Shin, H. S. Shin, G. Lee, Z. Lee, K. S. Kim, Multicomponent electrocatalyst with ultralow Pt loading and high hydrogen evolution activity, *Nat. Energy*, **2018**, *3*, 773-782.
- (34) L. Zhang, R. Si, H. Liu, N. Chen, Q. Wang, K. Adair, Z. Wang, J. Chen, Z. Song, J. Li, M. N. Banis, R. Li, T.-K. Sham, M. Gu, L.-M. Liu, G. A. Botton, X. Sun, Atomic layer deposited Pt-Ru dual-metal dimers and identifying their active sites for hydrogen evolution reaction. *Nat. Commun.*, **2019**, *10*, 4936.
- (35) T. Kim, S. B. Roy, S. Moon, S. Yoo, H. Choi, V. G. Parale, Y. Kim, J. Lee, S. C. Jun, K. Kang, S.-H. Chun, K. Kanamori, H.-H. Park, Highly Dispersed Pt Clusters on F-Doped Tin(IV) Oxide Aerogel Matrix: An Ultra-Robust Hybrid Catalyst for Enhanced Hydrogen Evolution, *ACS Nano*, **2022**, *16*, 1625–1638.
- (36) W. Yang, P. Cheng, Z. Li, Y. Lin, M. Li, J. Zi, H. Shi, G. Li, Z. Lian, H. Li, Tuning the Cobalt–Platinum Alloy Regulating Single-Atom Platinum for Highly Efficient Hydrogen Evolution Reaction, *Adv. Funct. Mater.*, **2022**, *32*, 2205920.
- (37) Q. Dong, S. Ma, J. Zhu, F. Yue, Y. Geng, J. Zheng, Y. Ge, C. Fan, H. Zhang, M. Xiang, Q. Zhu, Ultrahigh Mass Activity for the Hydrogen Evolution Reaction by Anchoring Platinum Single Atoms on Active {100} Facets of TiC via Cation Defect Engineering, *Adv. Funct. Mater.*, **2022**, *33*, 2210665.
- (38) Z. Zeng, S. Küspert, S. E. Balaghi, H. E. M. Hussein, N. Ortlieb, M. Knäbbeler-Buß, P. Hügenell, S. Pollitt, N. Hug, J. Melke, A. Fischer, Ultrahigh Mass Activity Pt Entities Consisting of Pt Single atoms, Clusters, and

Nanoparticles for Improved Hydrogen Evolution Reaction, *Small*, 2023, 19, 2205885.

(39) J. Park, S. Lee, H.-E. Kim, A. Cho, S. Kim, Y. Ye, J. W. Han, H. Lee, J. H. Jang, J. Lee, Investigation of the Support Effect in Atomically Dispersed Pt on  $\text{WO}_{3-x}$  for Utilization of Pt in the Hydrogen Evolution Reaction, *Angew. Chem. Int. Ed.*, **2019**, 58, 16038–16042.

(40) Y. Zhao, P. V. Kumar, X. Tan, X. Lu, X. Zhu, J. Jiang, J. Pan, S. Xi, H. Y. Yang, Z. Ma, T. Wan, D. Chu, W. Jiang, S. C. Smith, R. Amal, Z. Han, X. Lu, Modulating Pt-O-Pt atomic clusters with isolated cobalt atoms for enhanced hydrogen evolution catalysis, *Nat. Commun.*, 2022, 13, 2430.

(41) Y. Shi, Z.-R. Ma, Y.-Y. Xiao, Y.-C. Yin, W.-M. Huang, Z.-C. Huang, Y.-Z. Zheng, F.-Y. Mu, R. Huang, G.-Y. Shi, Y.-Y. Sun, X.-H. Xia, W. Chen, Electronic metal–support interaction modulates single-atom platinum catalysis for hydrogen evolution reaction. *Nat. Commun.*, 2021, 12, 3021.

(42) X. Cheng, Y. Li, L. Zheng, Y. Yan, Y. Zhang, G. Chen, S. Sun, J. Zhang, Highly active, stable oxidized platinum clusters as electrocatalysts for the hydrogen evolution reaction, *Energy. Environ. Sci.*, **2017**, 10, 2450-2458.

(43) X. Cheng, B. Xiao, Y. Chen, Y. Wang, L. Zheng, Y. Lu, H. Li, G. Chen, Ligand Charge Donation–Acquisition Balance: A Unique Strategy to Boost Single Pt Atom Catalyst Mass Activity toward the Hydrogen Evolution Reaction, *ACS Catal.*, 2022, 12, 5970–5978.